ISSN 1063-7710, Acoustical Physics, 2010, Vol. 56, No. 6, pp. 972–988. © Pleiades Publishing, Ltd., 2010.

Wave Propagation in Magnetic Nanofluids (A Review)

V. V. Sokolov

Moscow State University of Instrumentation and Computer Science, ul. Stromynka 20, Moscow, 107996 Russia
e-mail: vvs1953@rambler.ru

Received March 22, 2010

Abstract—Theoretical and experimental results on elastic wave propagation in magnetic nanofluids are presented. The theoretical results are compared with available experimental data on sound velocity anisotropy in magnetic nanofluids on various bases. A detailed description is given, using existing theories, of hydrodynamic modes of magnetized magnetic nanofluids, including new and predicted ones.

DOI: 10.1134/S1063771010060229

Ferrohydrodynamics is a comparatively new field of hydrodynamics, which emerged owing to the synthesis of magnetic colloids, called ferrocolloids, ferrofluids, magnetic fluids, and, in recent years, magnetic nanofluids (MNFs), since solid ferromagnet or ferrimagnet particles have a characteristic dimension of $d \sim 10$ nm [1]. At such a size, particles are single-domain and possess a magnetic moment $m_p = (\pi d^3 M_p)/6$, where M_p is the saturation magnetization of the magnet.

To prevent adhesion of particles due to dipole–dipole interaction, they are coated with a stabilizing layer, for instance, a surfactant, the choice of which is determined by the type of carrier liquid. In organic nonpolar liquids, one stabilizing layer is used, and in polar liquids, layers of various surfactants are used. Thus, an MNF is a multiphase medium, and the mixture of the stabilizer and carrier liquid is a dispersion medium. In terms of magnetic properties, a weakly concentrated MNF is similar to a superparamagnetic gas, the particle interaction in which is determined by the coupling constant $\lambda = m_p^2/d^3 k_B T$ characterizing the ratio of the dipole–dipole interaction of contacting particles to the energy of heat motion [2]. In strong magnetic fields at $H \gg m_p/d^3$, particles form particle chains parallel to the field [2]. MNF magnetization is described by the Langevin formula for a paramagnetic gas:

$$M = nm_p L(mH/k_B T), \quad L(\xi) = \coth\xi - \xi^{-1}.$$

The magnetization dynamics is determined by two fluctuation mechanisms [3]: the Néel relaxation time $\tau_N = \tau_0 \sigma^{-1/2} e^{\sigma}$, $\sigma = KV_p/k_B T$ as a result of heat fluctuations of the magnetic moment direction inside a particle with a volume V_p, the matter of which has an anisotropy constant K, and the Brownian time of rotational diffusion of the particle itself $\tau_B = 3V_p\eta/k_B T$ in a liquid with shear viscosity η.

In the physics of magnetic nanofluids, of significant interest is the problem of interparticle interactions and a number of questions relating to it: particle aggregation, the character of magnetic ordering, and the type of relaxation processes.

Physical acoustic methods are quite sensitive to structural features of matter and have a number of advantages in comparison to other methods. In particular, acoustic studies are conducted in the volume of matter without violating the structure, which makes it possible to trace the dynamics of processes occurring in matter.

First, we consider the experimental results on the acoustic properties of MNFs in the absence of external magnetic field. The first measurements of ultrasound velocity in MNFs were apparently conducted by the authors of [4], who established that addition, into a carrier liquid, of particles of a magnetic material lead to a decrease in ultrasound velocity, and the temperature dependence is determined by the carrier liquid. One year later, study [5] appeared, which contained only the ultrasound velocity value in kerosene (1275 m/s) and in an MNF based on it (1201 m/s). The results of a study by the authors of [6] were more substantive; they studied the results of the temperature influence on the propagation velocity of ultrasound in kerosene- and water-based magnetic fluids and established that the temperature coefficient of ultrasound velocity in kerosene-based magnetic fluids is negative when the volumetric content of magnetite varies in the range of 1.7–10.5%. In the case of a water-based MNF, the maximum on the temperature dependence of ultrasound velocity was discovered, the position of which changed with a change in the volumetric content of the magnet; the maximum of the ultrasound velocity in magnetic fluids was reached at a temperature lower than in distilled water. In [7], the ultrasound velocity in a kerosene-based MNF with various magnetite contents was also measured and, in accordance with previous studies, it was found that with an increase in

Table 1. Physical properties of a kerosene-based MNF

Sample	K_0	K_1	K_2	K_3	K_4	K_5	K_6	K_7
ρ, kg/m^3	795	879	1018	1103	1240	1325	1565	1767
$\eta \times 10^3$ Pa s	1.0	2.53	3.06	3.74	5.5	7.6	19.9	100.6
c, m/s	1320	1290	1215	1194	1150	1137	1098	1084
$(\alpha/f_1^2) \times 10^{15}$ s^2 m^{-1}	109	380	630	514	906	889	1210	1997
$(\alpha/f_2^2) \times 10^{15}$ s^2 m^{-1}	80	184	333	400	475	986	680	880
$(\alpha/f_3^2) \times 10^{15}$ s^2 m^{-1}		100	190	400		295		330

Table 2. Physical properties of a water-based MNF

Sample	B_0	B_1	B_2	B_3	B_4	B_5	B_6
ρ, kg/m^3	999	1022	1058	1104	1140	1197	1197
$\eta \times 10^3$ Pa s	1.0	1.11	1.23	1.51	1.97	2.43	2.48
c, m/s	1486	1477	1468	1445	1426	1420	1419
$(\alpha/f_1^2) \times 10^{15}$ s^2 m^{-1}	25	133	281	438	472	730	1265
$(\alpha/f_2^2) \times 10^{15}$ s^2 m^{-1}	25	71	84	1.59	185	230	182

the volumetric fraction of magnetite, the ultrasound velocity decreased nonlinearly. A more complete study of the concentration dependence of the ultrasound velocity in a kerosene-based MNF was conducted in [8]. Measurements were performed by the pulse-phase method at a frequency of 2.5 MHz. The volumetric content of magnetite and the studied samples changed in the range of 0–27.1%; the ultrasound velocity changed by 20%, and the wave impedance increased by almost a factor of 2. Work [9] presented the results of systematic studies of the propagation velocity of ultrasound in water-based MNFs, kerosene, and transformer oil with variation in temperature in the range 293–353 K. In all types of MNFs, it was observed that with increasing magnetite concentration, there was a decrease in the absolute value of temperature and concentration coefficients of ultrasound velocity.

Like in [6], a shift of the maximum in the temperature dependence of the propagation velocity of ultrasound in a water-based MNF was found; the higher the magnetite concentration, the greater the shift in the maximum in the lower temperature region. The first results of studying magnetic fluids by acoustic spectroscopy in the range of 3–50 MHz were presented in [10, 11]. Widening of the frequency range, in comparison to earlier works, made it possible to discover the relaxation character of ultrasound attenuation.

The physical properties of certain magnetite-type MNFs in kerosene (oleic acid was the stabilizer), studied in [10], are shown in Table 1 and correspond to a temperature of $T = 293$ K. These samples were prepared with the aim of determining the concentration dependences of the acoustic parameters by dilution with kerosene K_0 of concentrated sample K_7. The ultrasound velocity value corresponds to a frequency of $f_1 = 3.17$ MHz. The attenuation coefficient is also given for frequencies of $f_2 = 32.43$ MHz and $f_3 = 0.6$ GHz. The data in the last line of the table are taken from [12].

The ultrasound velocity is determined by the balance between the inertial and elastic properties of the medium. In weakly concentrated MNFs, magnetite particles coated by a stabilizing shell cause a significant change in density but do not much affect the condensability, so that the latter is close to the condensability of the carrier liquid. With an increase in concentration, interparticle interaction intensifies and therefore the assumption on the additivity of condensability is not satisfied. In the indicated frequency interval, the maximum dispersion of ultrasound velocity $\Delta c = 20$ m/s was found in sample K_7 at a temperature of 293 K. With growth in temperature, Δc decreased, and at $T = 333$ K, it was absent within the limits of measurement accuracy. We draw attention to the fact that at a frequency of 0.6 GHz, the attenuation coefficient in the samples with a small volumetric content of magnetite differed insignificantly from the attenuation coefficient in kerosene.

The properties of the studied water-based MNF samples [11] at $T = 293$ K are given in Table 2.

In samples B_1–B_5, the stabilizer was sodium oleate, and in sample B_6, it was a series of fatty acids; the solid phase in all samples was magnetite. It is noteworthy that the ultrasound velocity in samples B_5 and B_6 were

almost identical within the limits of measurement error, but the frequency dependences of the attenuation coefficient differed significantly; i.e., the attenuation coefficient was more sensitive to the MNF composition. This is possibly explained by the specifics of preparing water-based MNFs, since magnetite particles are coated by a double layer of various surfactants, and in order to ensure aggregate stability, a second layer of surfactants was added to the water. In [13, 14], experimental results were given on measuring the ultrasound attenuation coefficient at seven frequencies in the range of 3–40 MHz in water-based MNFs $\varphi = 0.357$ at three temperatures of 10, 20, and 30°C in the absence of external magnetic field. It was established that the ultrasound attenuation coefficient α/f^2 decreases nonlinearly with growth in frequency, and at a fixed frequency it decreases with increasing temperature. These data confirm the results given in [10].

For microinhomogeneous media, to which MNFs refer, there are two known energy dissipation channels of ultrasound waves caused by temperature equalization at the boundaries of two differently heated media during a periodic change in the temperature difference and a jump in velocity due to viscosity at the contact of media moving with a periodically changing difference in velocity. We consider a second dissipation channel, calling it the viscosity mechanism of ultrasound attenuation. An analysis of the applicability of this method to nonmagnetized magnetic fluids was given in [15].

Let a spherical particle of radius r with density ρ move at velocity v in a resting liquid having shear viscosity η. We estimate the relaxation time τ_0 related to equalization of the liquid and particle velocities. Writing the equation of particle motion in the form

$$\frac{4}{3}\pi r^3 \rho \frac{v}{\tau_0} = 6\pi r \eta v,$$

we obtain

$$\tau_0 = 2r^2\rho/9\eta. \quad (1)$$

This is the characteristic time parameter determining the presence of additional ultrasound attenuation in a dispersion medium, which apparently was first pointed out by the authors of the remarkable study [16]; as was shown in [15], the results [16] and subsequent studies [17–19] differed insignificantly. Additional attenuation of an ultrasound wave propagating in a viscous liquid in which spherical particles of a heterogeneous substance weigh greater, with a density differing from that of the medium, the smaller the period of the ultrasound wave in comparison to relaxation time τ. The main parameter in theory [16] is the ratio of particle radius r of the penetration depth of a viscous wave $\delta_\eta = \sqrt{2\eta/\rho_f\omega}$, i.e.,

$$\sqrt{\xi} = r/\delta_\eta. \quad (2)$$

Here, ρ_f is the density of the carrier liquid; ω is the cyclical frequency of the ultrasound wave. In writing the equation of motion, the authors of [16] use the Boussinesq formula for the force of friction acting on a particle vibrating in the ultrasound wave field. Attenuation coefficient α owing to the viscosity mechanism obtained in [16] has the form

$$\alpha = \frac{2}{9}\varphi a \frac{\omega}{c_f}\left(\frac{\rho_p}{\rho_f} - 1\right)^2 \frac{\xi(1+\sqrt{\xi})}{(1+\sqrt{\xi})^2 + \xi(1+b\sqrt{\xi})^2}, \quad (3)$$

where

$$b = \frac{2}{9}\left(1 + 2\frac{\rho_p}{\rho_f}\right). \quad (4)$$

Here, c_f is the velocity of ultrasound propagation in the carrier liquid. For small values of volumetric concentration φ of weighted particles $a = 1$.

In the foreign literature, [17] is usually considered a pioneering work on the viscosity mechanism. In this work, the Stokes formula is used for the force of friction acting on a particle in a; it describes a spherical pendulum oscillating in a viscous medium. Assuming that the dissipating energy of ultrasound is equal to the work of friction force, the author of [17] obtained the following expression for the ultrasound attenuation coefficient:

$$\alpha = \frac{\varphi}{2}\frac{\omega}{c_f}\left(\frac{\rho_p}{\rho_f} - 1\right)^2 \frac{s}{s^2 + \left(\frac{\rho_p}{\rho_f} + \tau^*\right)^2}, \quad (5)$$

where

$$s = \frac{9}{4}\frac{\delta_\eta}{r}\left(1 + \frac{\delta_\eta}{r}\right), \quad \tau^* = \frac{1}{2} + \frac{9}{4}\frac{\delta_\eta}{r}.$$

It is easy to see, with allowance for (2), that expression (5) coincides with Eq. (3) at $a = 1$.

As applied to MNFs, the viscosity mechanism of ultrasound attenuation was theoretically studied by the authors of [18], who in the case of spherically shaped particles obtained the expression for the attenuation decrement:

$$\delta^* = \frac{\varphi}{2}(1-\varphi)\frac{(\rho_p - \rho_f)^2}{\rho_p\rho_f}\omega\tau, \quad (6)$$

where

$$\tau = \frac{2}{9}\frac{r^2\rho_p}{\eta}\frac{(1-\varphi)\rho_f}{\rho}.$$

Note that this relaxation time τ differs from (1) by a factor on the order of unity. Since the viscosity mechanism of ultrasound energy dissipation lies at the base of theory [18], it then seems expedient to introduce into Eq. (6) in explicit form dimensionless parameter ξ determined by formula (2). After elementary trans-

formations with allowance for relation of the attenuation decrement to the attenuation coefficient $\alpha = \omega\delta^*/c_f$, Eq. (6) takes the form

$$\alpha = \frac{2}{9}\varphi a\frac{\omega}{c_f}\left(\frac{\rho_p}{\rho_f} - 1\right)^2\xi. \quad (7)$$

This expression for the attenuation coefficient is obviously a particular case of formula (3) at $\xi \ll 1$. Note that in this approximation and at $a = 1$, in [20] estimates are given for the contribution of the viscosity mechanism to ultrasound attenuation in an MNF. Results [18] were refined in [19], in which the following formula was given for the attenuation decrement:

$$\delta^* = \frac{1}{2}m^2\omega\tau\frac{Q}{Q^2 + S^2}, \quad (8)$$

where

$$Q = 1 + D_b\sqrt{\omega\tau}, \quad m^2 = \varphi\frac{(\rho_p - \rho_f)^2}{\rho_p\rho_f}, \quad D_b = \sqrt{\frac{k_\tau}{2}},$$

$$S = \sqrt{\omega\tau}[D_b + (1 + D_\lambda)\sqrt{\omega\tau}], \quad D_\lambda = \frac{k_\tau}{9},$$

$$k_\tau = \frac{9}{2}\frac{\rho}{(1-\varphi)\rho_p}.$$

As was shown in [15], these relations transform to

$$D_b\sqrt{\omega\tau} = \sqrt{\xi},$$

$$\frac{1}{2}m^2\omega\tau = \frac{2}{9}\frac{\varphi(1-\varphi)^2\rho_f}{\rho}\left(\frac{\rho_p}{\rho_f} - 1\right)^2\xi,$$

$$S = \left\{\frac{2}{9}\left[1 + 2(1-\varphi)\frac{\rho_p}{\rho}\right]\sqrt{\xi} + 1\right\}\sqrt{\xi};$$

therefore, expression (8) fully coincides with (3), but with the modified coefficient

$$\hat{b} = \frac{2}{9}\left[1 + 2(1-\varphi)\frac{\rho_p}{\rho}\right].$$

Calculations, performed in [15], of ultrasound attenuation with the help of relation (3) have shown that the viscous attenuation mechanism does not describe the experimental results for water-, kerosene-, and dodecane-based MNFs. The authors of [21] attempted to explain the velocity dispersion, discovered in [10], due to the viscosity mechanism [16]. For this, in [27], the particle size of magnetite was chosen such that the velocity dispersion value indicated in [10] was obtained. However, at the particle radius chosen in [21], ultrasound attenuation calculated using theory [16] exceeds that observed in experiments by almost a factor of 2, which was shown in [22].

The main difficulties in analyzing the acoustic spectrum of even nonmagnetized concentrated MNFs, which are non-Newtonian liquids, are related to violation of the additivity of the contributions of various ultrasound energy dissipation mechanisms, as well as with the absence of experimental data on the frequency dependence of shear viscosity. So, for instance, the use of shear viscosity values obtained at small shear velocity lead to an ultrasound attenuation coefficient that exceeds the experimental value. As is known, a similar situation takes place in polymer solutions.

We now consider the experimental results from studying the influence of magnetic field on the acoustic properties of MNFs. These results are quite important for the development of ferrohydrodynamics. Indeed, by now, despite the existence of a significant amount of continual models of nonconducting MNFs [23], there is still a tendency to construct new models [24–26]. This is based on the complexity of the modeled medium and the absence of criteria for the applicability of models. In this connection, study of the features of propagation of small-amplitude elastic waves in MNFs occupies a significant place in the development of ferrohydrodynamics, since the results of such studies make it possible now to appraise existing various ferrohydrodynamics equations in a linear approximation, under conditions of reliable experimental data, of course.

However, it has turned out historically that in one of the first experimental studies on measuring the influence of magnetic field on the propagation velocity of ultrasound in a water-based magnetic fluid [27] contained a methodical error. According to [27], the change in ultrasound velocity under the action of relatively weak fields (several hundred gauss) is 30–50%. These data have served as the basis for a number of inventions, for instance, of various generations of delay lines, the basis for criticism of theoretical studies on ultrasound propagation in MNFs. In [28], the methodical error in [27] was pointed out in the processing of experimental data. The authors of [27] used the phase method to determine the change in the ultrasound phase velocity in MNFs under the action of magnetic field; the essence of this method is measurement of the phase shift between two harmonic signals, one of which passes through an acoustic cell with the studied MNF, and the other, through a delay line. The phase velocity of an ultrasound wave c is related to simple formula with ultrasound frequency f, phase Φ_0, and acoustic-cell base length l,

$$c = 2\pi fl/\Phi. \quad (9)$$

Hence, it is easy to find that the relative change in ultrasound velocity as

$$\frac{\Delta c}{c} = \frac{\Delta\Phi}{\Phi_0}, \quad (10)$$

where $\Delta\Phi$ is the change in the phase during overlapping of the magnetic field. The authors of [27], using

relation (10), incorrectly chose Φ_0, assuming it equal to the phase shift $\Delta\Phi_0$ of the above-mentioned signals in the absence of magnetic field action. As well, the denominator in the formula (10) decreases by $2\pi n$, where n is the number of wavelengths λ stacked on acoustic base l. To evaluate reception, we take c equal to 1430 m/s and, according to [27], $l = 9.6$ mm, $f = 2.44$ MHz. The quantity $\Delta\Phi_0$ was determined from [29] by the same authors, which proved to be ~80°. Consequently, results [27] with the above-mentioned parameters were overstated by a factor of $1 + 2\pi n/\Delta\Phi_0 \sim 10^2$.

In [4], it was noted that no changes in propagation velocity of ultrasound were caused by homogeneous and inhomogenous fields of up to 600 E in intensity acting on a kerosene-based magnetic fluid. The authors of [9] using the phase method (1 MHz) and the pulse method (2.5 MHz), did not observe changes in the propagation velocity of ultrasound in MNFs based on kerosene, water, and transformer oil with a change in magnetic field strength to 40 kA/m. In [30], a study was conducted on magnetic field influence on the propagation velocity of ultrasound in kerosene-based MNFs with saturation magnetization of 48 kA/m. Without a field, the ultrasound velocity is 1135 m/s. In a magnetic field with a strength of 100 kA/m under collinear positioning of the weight vector and the vector of the magnetic field strength, the sound velocity was $c_l = 1139$ m/s, and with orthogonal orientation of the indicated vectors, $c_t = 1137$ m/s. It was noted in [31] that in water-based MNFs with a volumetric magnetite concentration of up to 8%, ultrasound velocity with variation in magnetic field strength from 0 to 380 kA/m does not change in either the longitudinal or latitudinal direction relative to the wave vector of the ultrasound wave.

There are two reasons for such contradictions in the data of various studies. First, the inadequacy of experimental methods of the problem being solved. So, in [4, 9, 30, 31], to determine the field dependence of ultrasound velocity in MNFs, the method of measuring the absolute value of ultrasound velocity was used. Naturally, the results of such measurements led to the conclusion on the absence of magnetic field influence on ultrasound velocity. In contrast, application of such methods seem quite acceptable if the results of pioneering study [27] are borne in mind.

The main problem that arose in measuring magnetic field influence on ultrasound velocity was determining conditions of the experiment that ensure reproducibility of the results. The authors of [27, 32] were the first to encounter this difficulty; to overcome it, they proposed subjecting a measurable sample of an MNF to periodic magnetic field action with an induction of 0.15–0.2 T. However, the use of this technique in our studies on the ultrasound velocity anisotropy have shown its invalidity, since the thus obtained experimental data had low reproducibility.

In [33], the dependence of ultrasound attenuation at a frequency of 2.25 MHz in water-based MNFs with variation in angle ϑ between the weight vector and the magnetic field direction was studied. The attenuation coefficient was measured for a fixed angle ϑ with an increase in magnetic field strength to 2.5 kG. It was discovered that at some angles, an increase in magnetic field strength leads first to an increase in attenuation; it then reaches a maximum at $H \sim 300$ G, after which it decreases and, passing through a minimum, again increases nonlinearly. However, at other angles, for instance, at $\vartheta = 70°$, the attenuation coefficient after switch-on of the magnetic field immediately begins to decrease, and after passing through a minimum, begins to increase. For a value of $H = 920$ G, a graph of the angle dependence of the ultrasound attenuation coefficient is given in [33]. As a consequence [32], these data are described by the formula

$$\alpha = 7.8\sqrt{(1+\sin^2\vartheta)}(1 - 2\sin^2\vartheta + 1.25\sin^4\vartheta); \quad (11)$$

as well, the following formula is given:

$$\alpha = 51\sqrt{\left(\frac{1+5\sin^2\vartheta}{1-0.5\sin^2\vartheta}\right)} \times \left(\frac{1-2.145\sin^2\vartheta+1.19\sin^4\vartheta}{1-0.5\sin^2\vartheta}\right),$$

which approximates the angle dependence of the ultrasound attenuation coefficient at a frequency of 6 MHz for the same MNF as in [33], but at $H = 450$ G.

Results were explained in [34] owing to the contribution of two mechanisms resulting in attenuation anisotropy. One was described by the expression for the attenuation coefficient and nematic liquid crystals, and the other was the viscosity mechanism. The author of [34] proposed that in an MNF, spherical aggregates formed from particles (with the same radius R, which later arrayed themselves in a chain along the magnetic field. The force of friction acting on an aggregate was described by the Stokes formula $F = -6\pi\eta R(v_a - v_f)$ (v_a, v_f are the vibration velocities of an aggregate and liquid particles, respectively; η is the shear viscosity of the carrier liquid. In addition, the force of elasticity of a chain of aggregates in a field was introduced ad hoc:

$$F = -\kappa\Delta x\sin\vartheta, \quad (12)$$

where ϑ is the angle between the weight vector of the ultrasound wave and the magnetic field direction, and Δx is displacement of the aggregate in the ultrasound wave. The ultrasound attenuation coefficient due to the viscosity mechanism was described by expression [34]:

$$\alpha = \frac{3\pi\eta R\omega^3 V_a n(6\pi\eta R + \rho_f V_a\omega)/c_f}{(\kappa\sin\vartheta - \rho_a V\omega^2)^2 + (6\pi\eta R\omega)^2}, \quad (13)$$

where V_a is the volume of the aggregate, c_f is the ultrasound velocity in the carrier liquid, and n is the number of aggregates in a unit of volume. Hence, at $\kappa = 0$, it follows that

$$\alpha = \frac{3\pi\eta R\omega^3 VN(6\pi\eta R + \rho_f V\omega)/c_f}{(\rho_a V\omega^2)^2 + (6\pi\eta R\omega)^2}. \quad (14)$$

This relation describes the contribution of only the viscosity mechanism of attenuation and therefore it should turn to zero in the limiting case corresponding to equality of the densities of the carrier liquid ρ_f and aggregate ρ_a. It is easy to see that expression (14) does not satisfy this requirement; therefore, formula (13) should be considered erroneous.

In [35], ultrasound attenuation in an MNF with ellipsoidal aggregates with an orthogonal orientation of the weight vector of the ultrasound wave and the magnetic field direction was studied. In addition to the viscosity mechanism, the contribution to ultrasound attenuation due to the presence of repulsion forces of a dipole nature between magnetized aggregates was considered.

Ultrasound attenuation in an MNF, the particle of the solid phase of which form the ellipsoidal aggregates, was considered in [36, 37]. It was supposed that ellipsoidal aggregates have equal size with a fixed value of the external magnetic field strength. The dipole moment of an aggregate was determined by the expression $p = 4M_p\pi a^2 b/3$, where quantities a and b are, respectively, the large and small semiaxes of an ellipsoidal aggregate; M_p is the saturation magnetization of matter of the solid phase of an MNF. It was supposed that the magnetic field strength was large enough that the long axes of ellipsoids were oriented along the magnetic field direction. Allowance was made only for forces of dipole repulsion between neighboring ellipsoids located at distance l, the size of which depends on temperature, the magnetic field strength, and the concentration of the solid phase. Propagation of an ultrasound wave at an angle of ϑ toward the magnetic field direction causes a shift in ellipsoid Δx; the repulsion forces due to dipole–dipole interaction $F_d = -\kappa\Delta x\sin\vartheta$, where $\kappa = 6\mu_0 p^2/\pi l^5$, tend to return an ellipsoid to its former location. Therefore, the restoring force (12) introduced in [34] has a dipole nature. For the force of friction acting on an ellipsoid vibrating with a velocity of v_a with a volume of V_a in an ultrasound wave, the Stokes formula was used:

$$F = -\rho_f V_a \tau \frac{d(v_a - v_f)}{dt} - \rho_f V_a \omega s(v_a - v_f),$$

where

$$\tau = L + \frac{9}{4}(\delta_\eta/b)K^2,$$

$$S = \frac{9}{4}(\delta_\eta/b)K^2(1 + (1/K))(\delta_\eta/a)K^2.$$

The angle dependences of inertial coefficient L entering into the expression for additional mass and friction coefficient K of an ellipsoidal aggregate with random orientation of its long axis relative to the weight vector of the ultrasound wave, were determined from symmetry notions by the relation

$$L = L_\parallel \cos^2\vartheta + L_\perp \sin^2\vartheta,$$

$$K = K_\parallel \cos^2\vartheta + K_\perp \sin^2\vartheta.$$

Quantities $L_\parallel$, $L_\perp$, $K_\perp$, $K_\parallel$ are given by the formulas presented in [38].

The ultrasound attenuation coefficient in an MNF with ellipsoidal aggregates is determined by the expression

$$\alpha = \frac{1}{2}\varphi\frac{\omega}{c_f}\frac{\left(\frac{\rho_a}{\rho_f} - 1 - \frac{\kappa\sin\vartheta}{\omega^2\rho_f V_a}\right)^2}{\left(\frac{\rho_a}{\rho_f} + \tau - \frac{\kappa\sin\vartheta}{\omega^2\rho_f V_a}\right)^2 + S^2} S. \quad (15)$$

It is interesting that when the densities of the aggregate and the carrier liquid are equal, formula (15) takes the form

$$\alpha = \frac{1}{2}\varphi\frac{\omega}{c_f}\frac{\left(\frac{\kappa\sin\vartheta}{\omega^2\rho_f V_a}\right)^2}{\left(\frac{\rho_a}{\rho_f} + \tau - \frac{\kappa\sin\vartheta}{\omega^2\rho_f V_a}\right)^2 + S^2} S.$$

This attenuation coefficient is based only on dipole interaction of neighboring aggregates, as a result of which the vibration velocity of aggregates in a sonic wave differs from that of the particles of the liquid. Experimentally, such a situation can take place in an emulsion based on an MNF. In another limiting case, at $\kappa = 0$, i.e., in the absence of dipole–dipole interaction, expression (15) coincides in accuracy with the formula for the attenuation coefficient calculated in [39]. In [40] the amplitude of the signal that passed through the MNF was measured from the magnetic field strength, and it was discovered that in a narrow range of values of magnetic field strength, ultrasound attenuation sharply increased.

Recently, there has been a tendency to study changes in ultrasound velocity and attenuation in nonequilibrium conditions due to overlapping of a magnetic field changing in time at a given rate. So, the authors of [41] measured the attenuation coefficient in a water-based MNF with a collinear and orthogonal magnetic field orientation with variation in the rate of magnetic field growth from 15 A m^{-1} s^{-1} to 1.5 kA m^{-1} s^{-1}, and they obtained rather various field dependences. However, in the majority of them, reso-

nance ultrasound attenuation was observed, which had been discovered earlier in [40]. The author of [42] experimentally studied the increase with a frequency of 1.6 MHz under magnetic field action on a water-based MNF, with various growth rates—16, 48, 136, 480 A m^{-1} s^{-1}—with collinear orientation of the magnetic field and wave vector. The maximum magnetic field strength was 80 kA/m. At all rates of growth in magnetic field strength, the increase in ultrasound velocity did not exceed 25 m/s, but the steady-state value of velocity was established more rapidly at a higher rate of growth in magnetic field strength. An interesting time dependence was discovered in [43], of the relative change in ultrasound velocity in a water-based MNF with a change in the magnetizing field to 530 mT with various rates of its growth. The observation time was determined by achievement of the indicated maximum induction. It turned out that at a rate of field growth of 5.30 mT/min, the ultrasound velocity reached a maximum after an hour, and then it began to decrease over the course of the entire observation time of ~100 min. At a maximum rate of field growth of 42.4 mT/min, ultrasound velocity increased linearly over the course of the entire measurement time of ~10 min.

In [44], angle dependences of the attenuation coefficient were obtained for a water-based MNF with overlapping of the external magnetic field, the growth rate of which was 200 A m^{-1} s^{-1}. The field dependences of attenuation were determined at a fixed angle ϑ. Anisotropy of attenuation $\Delta\alpha = \alpha(\vartheta) - \alpha(\pi/2)$ with growth in the magnetic field strength increased monotonically, and the maximum value was $\Delta\alpha \sim 2$ m^{-1}.

The authors of [45] proposed a new mechanism of ultrasound energy dissipation in magnetized MNFs due to vibration of two particles (dimers) in a viscous medium, the change of the mean distance between which had a relaxation character and depended on the angle formed by the dimer axis and the wave vector of the ultrasound wave. Using this mechanism, experimental results [44] were explained. The angle dependence of a normalized attenuation coefficient was calculated by the formula

$$\frac{\alpha(\vartheta)-\alpha(\pi/2)}{\alpha(0)-\alpha(\pi/2)} = \frac{2(1-S)\cos^2\vartheta + 3S\cos^4\vartheta}{2+S}, \quad (16)$$

where $S(\lambda, \xi)$ is the order parameter. The right-hand side of this expression is a nonnegative function at all allowable values of the parameters entering into it; therefore, using this mechanism, it is impossible to explain experimental results [32, 33].

The kinetics of structural changes in a kerosene-based MNF located in an inhomogeneous magnetic field was studied in [46]. When a magnetic field is switched on that is collinear to the wave vector, the ultrasound attenuation coefficient increases slowly, reaching a maximum value which weakly depends on the field strength. Further the coefficient decreases insignificantly and then again increased up to achieving a constant value. When the field was switched off, the attenuation coefficient to a smaller value in comparison to its initial one in the absence of field. The strength of $H < 60$ kA/m, the ultrasound attenuation coefficient having passed through a maximum, increased to the value at the moment the field was turned on.

The time it takes to achieve a maximum and a constant value of attenuation depends on the field strength, growing as it decreases: at 118 kA/m, it is ~230 s; at 90 kA/m, ~260 s; and at 60 kA/m, 280 s. A repeat of the results was achieved after intense mixing of the liquid. With repeat overlapping of the magnetic field, a sharp maximum of the attenuation coefficient was observed, significantly depending on the magnetic field strength. Further, attenuation decreased and, having passed through a minimum, increased to a certain constant value, also depending on H. The time it takes for a constant value of the attenuation coefficient to be established decreases with an increase in magnetic field strength; however, this time is significantly less than for the initial sample. Subsequent switch-ons of the magnetic field with changing intensity did not change the character of ultrasound attenuation behavior. Switching off the field led to a decrease in attenuation to the initial level within several seconds, which apparently is explained by recession of chains from the region of the ultrasound beam. In this connection, it seemed expedient to measure the acoustic parameters in equilibrium conditions, which allowed the formation of particle chains and their distribution in the volume of the liquid.

These structural changes are determined by diffusion processes, for the completion of which, as it turned out, sufficiently large time intervals are required. The specifics of MNFs were accounted for by the fact that the magnetic field was created with permanent magnets, since it had been experimentally established that the holding time of the MNF sample in the field, ensuring reproducibility of results, were tens and hundreds of hours. To obtain the angle dependences of the acoustic properties, permanent magnets were set up on a rotating platform. Thermostatting of the measuring cell was ensured with an accuracy of ∓ 0.05. In [47] experimental results were presented on the anisotropy of ultrasound velocity and attenuation in kerosene- and dodecane-based MNFs, measured at a frequency of 2.7 MHz. Magnetization of samples was carried out in the field of a permanent magnet with an intensity of 2.7 kG with variation in temperature from 293 to 333 K.

Figure 1 shows the anisotropy of velocity in a kerosene-based MNF at 293 K. The exposure time of the sample in a magnetic field was about 100 h. Figure 2 shows the dependence of the anisotropy of ultrasound velocity in an dodecane-based MNF at 293 K for two

cases: squares correspond to an MNF located in a magnetic field for 10 h, and circles, for 200 h.

The frequency dependence of anisotropy of the propagation velocity of ultrasound was measured in a water-based MNF, the stabilization of colloid particles in which was carried out with sodium oleate [48]. The main parameters of the magnetic fluid were as follows: saturation magnetization, 12 kA/m; density, 1148 kg/cm^3; and ultrasound velocity in a nonmagnetized state, 1481 m/s. The values of these parameters correspond to a temperature of 293 K. Before measurements were begun, the acoustic cell with the magnetic fluid was kept in a magnetic field with a strength of 2.7 kG for about 50 h, and then measurements were conducted. The experimental results, presented in Fig. 3, correspond to a temperature of 293 K.

As is seen, the frequency dependence of anisotropy of the ultrasound velocity manifests itself the most distinctly at small angles ϑ. In recent work [49], the dependence of anisotropy on frequency in water- and kerosene-based MNFs was measured.

Figure 4 shows the anisotropy of the ultrasound attenuation coefficient. Triangles correspond to a kerosene-based MNF; measurements were conducted at 333 K [47]. Experimental data denoted by circles were obtained for a water-based MNF with holding in 1.5-kG magnetic field for about 150 h, after which reproducibility of results was achieved [50]. However, with a change in angle ϑ, a non-steady-state behavior of amplitude of the received signal was observed; only after 3–10 min did the signal level achieve a constant value, which was measured in experiment [50].

The angle dependences of ultrasound attenuation and velocity in a water-based MNF depend on the particle concentration of the magnet [51]. In a 1.5-kG magnetic field in a weakly concentrated MNF, the ultrasound velocity and attenuation coefficient monotonically increase with an increase in angle ϑ, reaching a maximum at $\vartheta = \pi/2$. In a concentrated MNF under the same experimental conditions, these dependences have a directly opposite character [51]. Note that these experimental data cannot be explained using the attenuation mechanism suggested in [45].

In [5], the field dependences of the ultrasound velocity anisotropy in a water-based MNF with a density of 1380 kg/m^3, a magnetite mass particle concentration of 40%, and saturation magnetization of 38 mT were obtained for the first time. The anisotropies of ultrasound velocity with a frequency of 1 MHz were measured for four values of induction of the magnetizing field: 50, 150, 250, and 350 mT at a fixed temperature of 293 K. The character of the angle dependences relative to the change in velocity changed with an increase in field. Figure 5 shows the experimental data (circles) at B = 50 mT, and Fig. 6, at B = 350 mT [52]. These data were theoretically described in [53], and the results of calculations are shown by solid lines in Figs. 5 and 6.

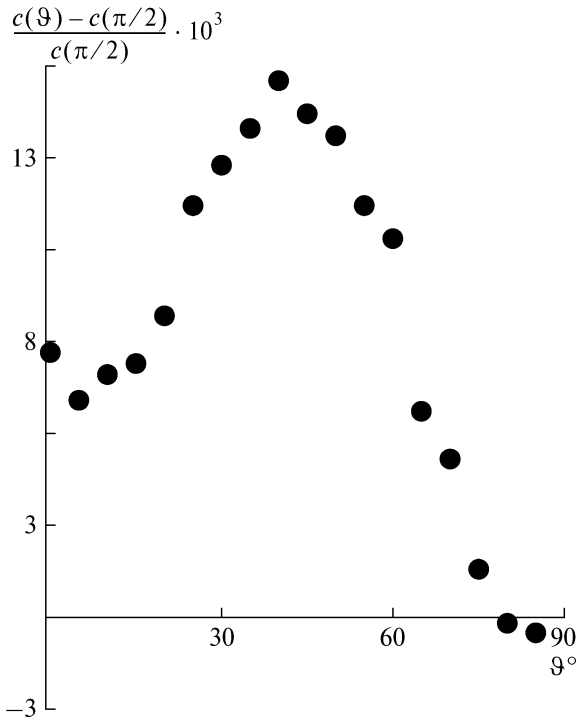

Fig. 1. Anisotropy of ultrasound velocity in a kerosene-based MNF.

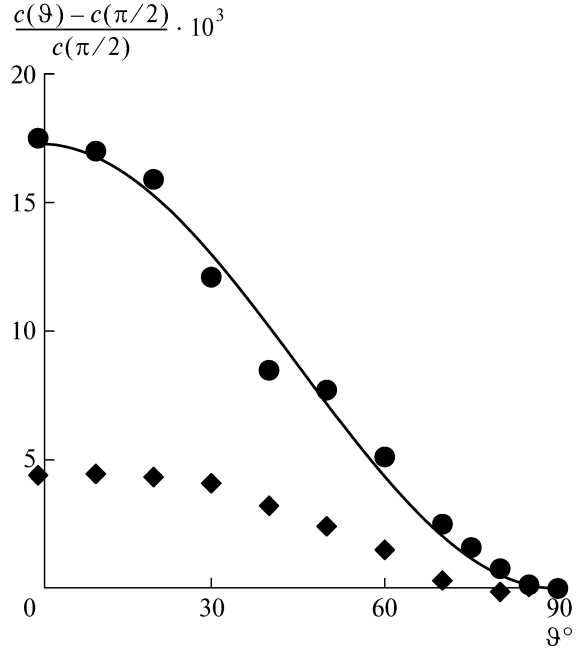

Fig. 2. Anisotropy of ultrasound velocity in an dodecane-based MNF.

Generalizing the obtained experimental results, we can highlight four types of angle dependence of ultrasound velocity: (1) the velocity reaches a maximum with parallel orientation of the wave vector and mag-

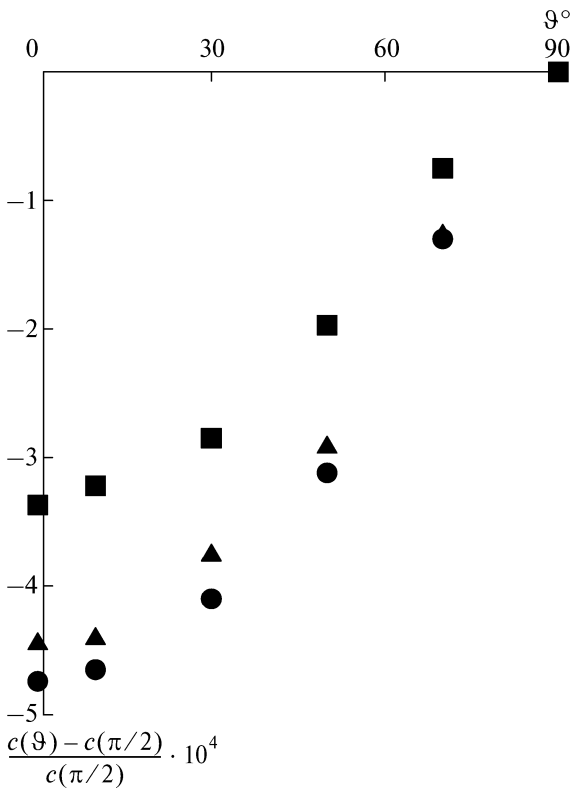

Fig. 3. Frequency dependence of anisotropy of ultrasound propagation in a water-based MNF.

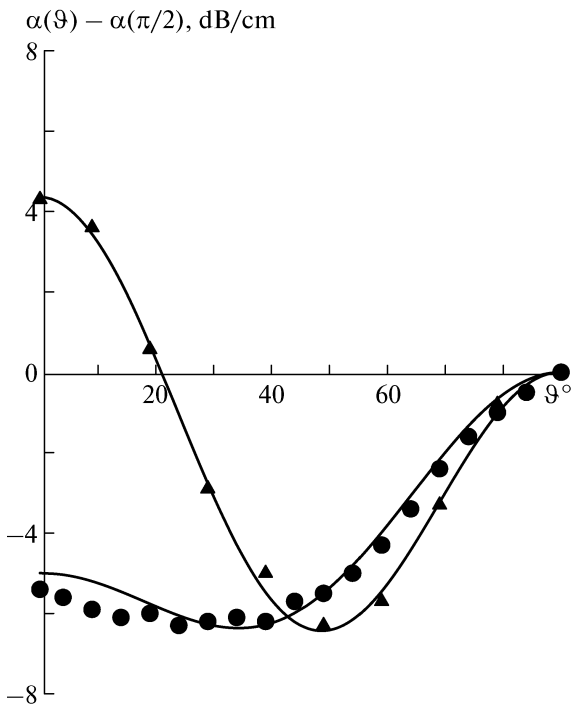

Fig. 4. Anisotropy of ultrasound attenuation in kerosene- and water-based MNFs.

netic field direction, and the minimum is reached with orthogonal orientation; (2) the velocity reaches a maximum also with parallel orientation of the wave vector and the magnetic field direction, but it reaches a minimum at an orientation that differs from orthogonal; (3) the velocity has a maximum at a certain orientation differing from parallel and orthogonal; (4) the velocity reaches a maximum with orthogonal orientation, and the minimum is reached with parallel orientation.

Therefore, we can conclude that at least two mechanisms making opposite contributions are responsible for the anisotropy of ultrasound velocity in magnetized magnetic fluids.

Thus, the experimental data known to date on magnetic field influence on ultrasound velocity in an MNF confirm the conclusion of [28] on the methodical error committed by the authors of [27], since the 100-fold decreased data [27] agree with the data presented above. Further we consider the results of theoretical studies of magnetic field influence on the acoustic properties of MNFs.

The relaxation mechanism of sound attenuation in an MNF due to the finiteness of the time of the establishment of equilibrium magnetization was suggested by the authors of [54], who considered the case of collinear orientation of wave vector of the sound wave and the magnetic field strength and obtained the following relations or the attenuation coefficient,

$$\alpha_\tau = \frac{(c_\infty^2 - c^2)}{2c_0^3}\frac{\omega^2\tau}{(1+\omega^2\tau^2)} \tag{17}$$

and for sound velocity,

$$c^2 = c_0^2 + \frac{4\pi M^2}{\rho(1+12\pi\chi L')},$$

where the following notation was introduced: $\tau = \tau_B/(1+12\pi\chi L')$, χ is susceptibility; L' is the derivative of the Langevin function; c_∞ is the velocity of sound in the high frequency limit, equal to

$$c_\infty^2 = c_0^2 + \frac{4\pi M^2}{\rho}.$$

Hence it follows that the maximum relative change in sound velocity is

$$\frac{\Delta c}{c_0} = \frac{2\pi M^2}{\rho c_0^2}. \tag{18}$$

For an estimate, we put $M = 100$ G, $\rho = 1$ g/cm^3, $c_0 = 10^5$ cm/s and find that the maximum relative increase in ultrasound velocity is 6×10^{-6}.

At present, the main theory describing the dynamic processes in MNFs is ferrohydrodynamics with allowance for internal rotation. In [55], to determine the spectrum of eigenmodes of an MNF having an inter-

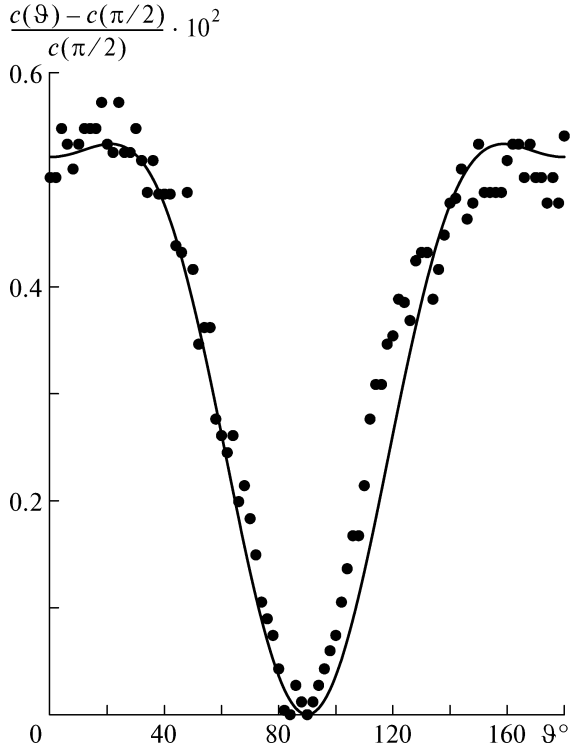

Fig. 5. Anisotropy of ultrasound velocity in a water-based MNF at $B = 50$ mT.

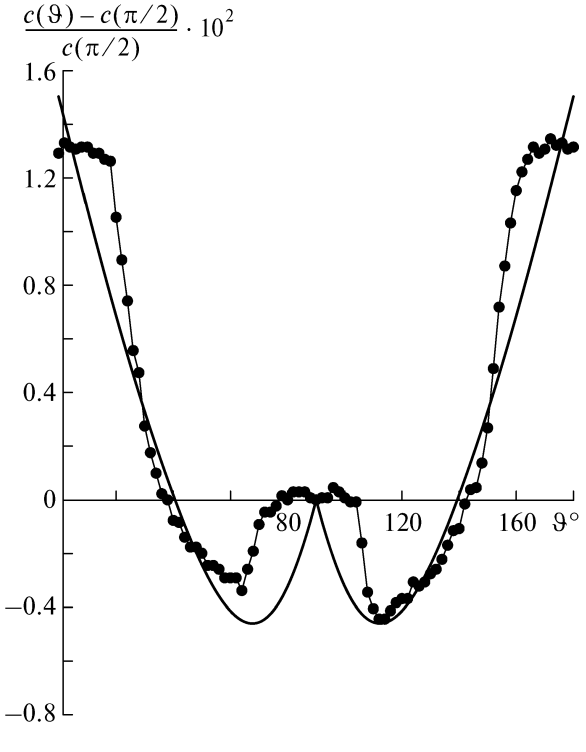

Fig. 6. Anisotropy of ultrasound velocity in a water-based MNF at $B = 350$ mT.

nal angular momentum $\mathbf{S}$, the following system of equations were used, which was obtained in [56, 57]:

$$\rho\left[\frac{\partial \mathbf{v}}{\partial t} + (\mathbf{v}\nabla)\mathbf{v}\right] = -\nabla p - \nabla\left[\frac{\mathbf{S}}{I}(\mathbf{S} - I\boldsymbol{\Omega})\right]$$

$$+ (\mathbf{M}\nabla)\mathbf{H} + \eta\Delta\mathbf{v} + \frac{1}{2\tau_s}\nabla\times(\mathbf{S} - I\boldsymbol{\Omega}),$$

$$\frac{\partial \rho}{\partial t} + \nabla(\rho\mathbf{v}) = 0,$$

$$\frac{\partial \mathbf{M}}{\partial t} + (\mathbf{v}\nabla)\mathbf{M} \qquad (19)$$

$$= -\frac{1}{\tau_B}\left(\mathbf{M} - M_e\frac{\mathbf{H}}{H}\right) - \frac{1}{I}\mathbf{M}\times\mathbf{S} - \mathbf{M}\nabla\mathbf{v},$$

$$\frac{\partial \mathbf{S}}{\partial t} + (\mathbf{v}\nabla)\mathbf{S} = -\frac{1}{\tau_S}(\mathbf{S} - I\boldsymbol{\Omega}) + \mathbf{M}\times\mathbf{H} - \mathbf{S}\nabla\mathbf{v},$$

$$\nabla\times\mathbf{H} = 0, \quad \nabla\mathbf{H} + 4\pi\mathbf{M} = 0.$$

Here, I is the moment of inertia of particles contained in a volume unit of a liquid; τ_S is the time of particle rotation decay in a viscous liquid; and $2\boldsymbol{\Omega} = \nabla\times\mathbf{v}$. In the ultrasound frequency region, the inequality $\omega\tau_S \ll 1$ is justified, which makes it possible to ignore particle spin and to use the steady-state equation in order to determine the internal angular momentum:

$$\mathbf{S} + \tau_S\nabla(\mathbf{v}\cdot\mathbf{S}) = I\boldsymbol{\Omega} + \tau_S\mathbf{M}\times\mathbf{H}. \qquad (20)$$

Using system of equations (19) with allowance for (20), the authors of [55] studied the propagation of small perturbations in an MNF with an internal angular momentum. They established that with orthogonal orientation of the wave factor of a sound wave and magnetic field intensity H, the velocity and decrement of attenuation δ of ultrasound do not depend on intensity, but with parallel orientation of the indicated vectors, the rate and decrement of attenuation δ are given by the relations

$$c = c_0\left[1 + \frac{8\pi\chi(\Omega_A\tau_B)^2}{(1+4\pi\chi_d)^2 + (\omega\tau_B)^2}\right], \qquad (21)$$

$$\delta = \frac{8\pi(1+4\pi\chi_d)\chi(\Omega\tau_B)^2}{\tau_B[(1+4\pi\chi_d)^2 + (\omega\tau_B)^2]}. \qquad (22)$$

So, the sound velocity has a relaxation character, and the timescale is determined by the Brownian time of orientational relaxation of magnetic moment τ_B. The dependence on magnetic properties is determined by the static χ and differential χ_d magnetic susceptibili-

ties. Introducing notation $\tau = \tau_B/(1 + 4\pi\chi_d)$, we rewrite the above-mentioned relations in the form

$$c = c_0\left[1 + \frac{2\pi M^2}{\rho c_0^2}\frac{\omega^2\tau^2}{(1+\omega^2\tau_B^2)}\right], \quad (23)$$

$$\alpha = \frac{2\pi M^2}{\rho c_0^3}\frac{\omega^2\tau}{(1+\omega^2\tau^2)}. \quad (24)$$

The obtained attenuation coefficient (24) corresponds in accuracy with (17). The relative increase in sound velocity in the high frequency limit $\omega\tau \gg 1$ corresponds to (18). For further explanation, the Alfven frequency $\Omega_A = \sqrt{\chi/4\rho}\,Hk$ found in [55] is of interest; as well, the authors note that in fact there is no Alfven branch in a magnetic fluid due to strong attenuation. Therefore, frequency Ω_A only characterizes interaction modes of various type. Nevertheless, we write the expression for the propagation velocity of an Alfven mode:

$$c_A = \sqrt{\frac{\chi}{4\rho}}H. \quad (25)$$

The authors of [58] especially emphasized the importance of experimental and theoretical study of the anisotropy of the acoustic properties of magnetic fluids, since precisely study of the anisotropy of acoustical properties allows one to make a substantiated choice between the following two equations of magnetization motion for an ideal MNF:

$$\frac{\partial M_i}{\partial t} + (\mathbf{v}\cdot\nabla)\mathbf{M} + \frac{1}{2}\mathbf{M}\times(\nabla\times\mathbf{v}) = 0, \quad (26)$$

and

$$\frac{\partial \mathbf{M}}{\partial t} + \nabla\times(\mathbf{M}\times\mathbf{v}) + \mathbf{v}(\nabla\cdot\mathbf{M}) = 0. \quad (27)$$

If magnetization changes in accordance with (26), then the dependence of sound velocity on magnetic field is determined by the expression

$$c^2 = c_0^2 - \frac{H_0^2}{8\pi}\left[(2+\gamma)\left(\frac{\partial\mu}{\partial\rho}\right)_T + \gamma\rho\left(\frac{\partial^2\mu}{\partial\rho^2}\right)_T\right], \quad (28)$$

which contains the contribution due to be magnetostriction effect:

$$c^2 = c_0^2 - \frac{\gamma H_0^2}{8\pi}\left[\left(\frac{\partial\mu}{\partial\rho}\right)_T + \rho\left(\frac{\partial^2\mu}{\partial\rho^2}\right)_T\right]. \quad (29)$$

Here $\gamma = C_p/C_V$ and μ is magnetic permeability. As is seen from (28), the sound velocity in this case is isotropic. If Eq. (27) is justified, then the sound velocity should be anisotropic, and with collinear orientation of the wave vector and magnetic field direction, it is described by expression (29), and with orthogonal orientation, by expression (28).

The magnetostrictive mechanism of anisotropy of ultrasound velocity was considered in [59], where the following relation was obtained, which describes the anisotropy of sound velocity:

$$c^2 = c_0^2 + \frac{4\pi M^2}{\rho}\left[1 + \frac{\rho}{\chi}\left(\frac{\partial\chi}{\partial\rho}\right)_0\right]\cos^2\vartheta, \quad (30)$$

from which follows

$$\frac{\Delta c}{c_0} = \frac{2\pi M^2}{\rho c_0^2}\left[1 + \frac{\rho}{\chi}\left(\frac{\partial\chi}{\partial\rho}\right)_0\right]\cos^2\vartheta. \quad (31)$$

Note that formula (30) leads to an increase in ultrasound velocity due to magnetostriction, which contradicts the conclusion of [58]. The maximum value of the relative increase in ultrasound velocity determined by relation (31) at $\vartheta = 0$ coincides with (18).

In [60], the following relation was the result of theoretical study of magnetic field influence on the sound propagation velocity in an MNF:

$$c^2 = c_0^2 - \frac{\mu M^2}{\rho}\left[\frac{1-\cos^2\vartheta}{1-\left(\chi - \mu\frac{M}{B}\right)\cos^2\vartheta}\right], \quad (32)$$

which predicts the maximum value of the relative decrease in ultrasound velocity, coinciding in modulus with (18).

The authors of [61], using the theory that uses (26) to describe the magnetization motion, highlighted the following relation to take into account the effect of the magnetic field on ultrasound velocity:

$$c^2 = c_0^2 - \frac{\mu_0 M^2}{\rho\chi}\left[\left(\frac{\rho}{\chi}\frac{\partial\chi}{\partial\rho}\right)^2\frac{\chi}{1+\chi}\cos^2\vartheta - \left(\frac{\rho^2}{2\chi}\frac{\partial^2\chi}{\partial\rho^2}\right)\right], \quad (33)$$

which according to its estimate gives a relative change in sound velocity significantly smaller than 10^{-4}.

The analogy of magnetic fluids to nematic liquid crystals was first used in [62]. The role of a director in the case of an MNF was played by a unit vector directed along the magnetization vector. However, in contrast to liquid crystals, in the equation of director motion, the inertial component was taken into account, which in the final analysis resulted in the existence within this theory of so-called natural resonance, the frequency of which is $\omega_c = \sqrt{m_0 H/I}$, where m_0 is the magnetization density, I is the density of the moment of inertia, and H is the magnetic field strength. Another characteristic time parameter appeared in theory [62] as a result of allowance, in the equation of director motion, of the rotation moment caused by the viscosity and determined with the vis-

cosity coefficients of torsion in velocity gradient γ_1 and γ_2 ($\lambda = \gamma_1/\gamma$). The time of relaxation of director fluctuations τ is given by the formula $\tau = \gamma_1/m_0 H$. The dependence of sound velocity on the size and direction of magnetic field magnetization is described by the relation

$$c = c_0\left(1 + \varphi\frac{\lambda^2\gamma_1\omega}{\rho_0 c_0^2}\left(1 - \frac{\omega^2}{\omega_0^2}\right)\right.$$
$$\left.\times\left\{\frac{\omega\tau}{\left[\left(1 - \frac{\omega^2}{\omega_0^2}\right)^2\right] + \omega^2\tau^2}\right\}\sin^2 2\vartheta\right). \quad (34)$$

For the attenuation coefficient, the following expression was obtained in [62]:

$$\frac{\omega}{\omega^2} = \varphi\frac{\lambda^2\gamma_1\omega}{8\rho_0 c_0^2}\left(1 - \frac{\omega^2}{\omega_0^2}\right)$$
$$\times\left\{\frac{\omega\tau}{\left[\left(1 - \frac{\omega^2}{\omega_0^2}\right)^2\right] + \omega^2\tau^2}\right\}\sin^2 2\vartheta. \quad (35)$$

According to the author of [62], at $\omega\tau \gg 1$, from (34) it follows that the relative increase in ultrasound velocity is 10^{-4}–10^{-5}.

An analogy of a magnetic fluid to a nematic liquid crystal was also made by the author of [63] with the aim of obtaining ferrohydrodynamic equations with an internal angular momentum. However, in this, a totally unsubstantiated assumption on equality of parameter λ to zero is made, the consequence of which was the disappearance of anisotropy of the acoustic properties of a magnetic fluid within the framework of theory [62] (see also (34) and (35)). In addition, the authors of [63] introduced, without substantiation, the Frank modulus (torsion modulus) for a magnetic fluid. Study [64] contains the opposite conclusion: there are no torsion moduli in a magnetic fluid, and parameter $\lambda \neq 0$. In [64] yet another system of ferrohydrodynamic equations was introduced precisely to explain the anisotropy of the acoustical properties of a magnetic fluid. It is supposed that a chain of magnetic particles in a magnetic field possesses elastic properties characterized by elasticity coefficient χ^*. This elasticity arises owing to balance of forces acting between particles, namely: dipole–dipole interaction results in particle attraction to each other, and their repulsion occurs due to the presence of surfactant shells on the particle surface. The results of [64] reduced to the following equations for angle dependences: ultrasound velocity,

$$c^2 = c_0^2 + \frac{\chi^* m_0^2}{\rho_0}\cos^4\vartheta, \quad (36)$$

and attenuation decrement,

$$\delta = \frac{\chi^* m_0^2}{\rho_0 c_0^3 \omega\tau_m}\cos^4\vartheta. \quad (37)$$

Here, τ_m denotes the time of relaxation of magnetization, and m_0 denotes the magnetization density. A new hydrodynamic mode introduced in [64] is of interest, which the authors call magnetoelasticity; it propagates at a velocity of

$$v = m_0\sqrt{\chi^*/\rho_f}. \quad (38)$$

Thus, the theoretical results listed above on the influence of magnetic field on ultrasound velocity differ from experimental results by three orders. In this connection, a new approach to ferrohydrodynamics was proposed, based on the concept of frozen-in of magnetization. To derive ferrohydrodynamic equations, the generalized principle of virtual displacements for continuous heat-conducting magnetized media was applied in the formulation of V.V. Tolmachev [65]:

$$\delta(U - T_0 S + p_0 V + W)$$
$$= \int_V \rho(f_i\delta^* q_i)dV + \int_{\partial V}(F_i\delta^* q_i)d\sigma. \quad (39)$$

Given variational equation is satisfied for a continuous body of volume V limited by surface ∂V placed into a thermostat with temperature T_0 at a fixed external pressure p_0 and is justified with random virtual shifts $\delta^* q_i$ from a position of equilibrium. Here, U, S, W denote the internal energy, entropy, and magnetic field energy, respectively; **f** represents volumetric forces; and **F** represents surface forces. Symbol δ^* stands for Lagrange variation. This principle makes it possible to isolate from among possible virtual states of a continuous body that state which in fact is equilibrium under the given external conditions. A distinct feature of the indicated variational principle is consideration of the finite volume of a continuous body, which makes it possible to obtain equilibrium conditions not only in the volume, but also on the surface.

The ferrohydrodynamic equations were introduced for two limiting cases. One corresponds to the assumption on equilibrium magnetization of a magnetic fluid [66]; i.e., the relaxation time of magnetization to an equilibrium value was assumed to be infinitely small.

The obtained equations coincided with the equations of quasi-steady-state ferrohydrodynamics. However, in deriving these equations, a new condition of thermodynamic equilibrium of an MNF in an external magnetic field **H** was obtained:

$$\mathbf{H} = \left(\frac{\partial \epsilon}{\partial \mathbf{m}}\right), \tag{40}$$

which means that, in the state of thermodynamic equilibrium in the neighborhood of any point of the liquid, the magnetic field strength is equal to the thermodynamic equilibrium strength, determined by the relation

$$\mathbf{H}^{\text{eq}} = \left(\frac{\partial u}{\partial \mathbf{m}}\right)_{\rho, s}. \tag{41}$$

This condition of magnetic equilibrium in essence represents the general form of the material equation for the electrodynamics of a continuous medium with allowance for its thermodynamic properties. Indeed, using the known function of specific internal energy ϵ, from the condition of magnetic equilibrium follows the relationship between magnetization of the medium and the magnetic field strength [66]. A similar result was obtained in describing the dynamic processes of magnetization of an MNF [24]. A similar interpretation of the material relation for dielectrics was given in [67]. Another limiting case corresponded to the assumption of freezing magnetization into a magnetic fluid [68]; here, the relaxation time of magnetization of a magnetic field to an equilibrium value is infinitely large. The equation for frozen-in of magnetization has the form

$$\frac{d\mathbf{M}}{dt} = (\mathbf{M}\cdot\nabla)\mathbf{v} - \mathbf{M}\nabla\cdot\mathbf{v}, \tag{42}$$

which with allowance for the continuity equation can be rewritten for a specific magnetization:

$$\frac{d\mathbf{m}}{dt} = (\mathbf{m}\cdot\nabla)\mathbf{v}. \tag{43}$$

Note that equation of motion (27) applied in [58] is the equation of frozen-in of magnetization and after simple transformations coincides with (42). Equation (43) in form and accuracy coincides with the equation of frozen-in for a specific intensity of a magnetic field in an ideal liquid with infinite conductivity [69]. The physical grounds for introducing this limiting case was description of dynamic processes, in particular, ultrasound propagation in an MNF. Using the data of Tables 1 and 2, we can confirm that ultrasound attenuation α at wavelength λ satisfies the inequality $\alpha\lambda \ll 1$; therefore, to take into account the influence of external magnetic field on ultrasound velocity, an approximation of an ideal liquid was used. A complete system of equations was given in [70] for a magnetic fluid with frozen-in magnetization with allowance for dissipative processes, in particular, finiteness of the relaxation time τ of magnetization of a magnetic field to an equilibrium value. In this case, equation of motion of magnetization (43) changes due to the addition of the relaxation term

$$\rho\frac{d\mathbf{m}}{dt} = \rho(\mathbf{m}\cdot\nabla)\mathbf{v} + \frac{\mathbf{H}-\mathbf{H}^{\text{eq}}}{\tau}. \tag{44}$$

The system of equations describing an ideal nonconducting MNF of density ρ with frozen-in magnetization $\mathbf{M} = \rho\mathbf{m}$ and which moves at velocity **v** includes the following equations [68]:

$$\begin{gathered}
\frac{\partial\rho}{\partial t} + \frac{\partial(\rho v_j)}{\partial x_j} = 0,\\
\rho\frac{\partial v_i}{\partial t} = -\frac{\partial P}{\partial x_i} + (H_i^{\text{eq}} - H_i)\frac{\partial(M_j)}{\partial x_j} + M_k\frac{\partial H_i^{\text{eq}}}{\partial x_k},\\
\frac{dm_i}{dt} = m_j\frac{\partial v_i}{\partial x_j},\\
\frac{\partial s}{\partial t} + v_i\frac{\partial s}{\partial x_i} = 0,\\
H_i^{\text{eq}} = \left(\frac{\partial\epsilon}{\partial m_i}\right)_{\rho, s}, \quad p = \left(\rho^2\frac{\partial\epsilon}{\partial\rho}\right)_{s, m},\\
H_i = -\frac{\partial\Psi}{\partial x_i}, \quad \nabla^2\Psi = 4\pi\frac{\partial(\rho m_j)}{\partial x_j}.
\end{gathered} \tag{45}$$

The last two equations of the system are the magnetostatic Maxwell equations, where Ψ is the scalar potential of the magnetic field. The system is closed by assigning the function of specific internal energy $\epsilon = \epsilon(\rho, s, \mathbf{m})$. In [71], the Hamiltonian form of these equations is given.

With linearized system of equations (45), the hydrodynamic modes of an MNF with frozen-in magnetization were obtained [72, 73]. Expansion of the internal energy near the background state had the form

$$\epsilon(\rho, s, \mathbf{m}) = \epsilon_0 + \beta_{ij}m_i m_j + \alpha_k m_k\rho, \tag{46}$$

where

$$\beta_{ij} = \frac{1}{2}\left(\frac{\partial^2\epsilon}{\partial m_i\partial m_j}\right)_{\rho, s}, \quad \alpha_k = \frac{1}{2}\left(\frac{\partial^2\epsilon}{\partial m_k\partial\rho}\right)_s.$$

Phenomenological coefficients β_{ij} and α_k characterize the magnetoelastic and magnetostrictive properties, respectively. In solving linearized system (45), the external magnetic field is assumed to be directed along the z axis; therefore, in this geometry, tensor β_{ij} is diagonal with the components $\beta_{xx} = \beta_{xx} = \beta_\perp$, $\beta_{zz} = \beta_\parallel$; vector $\boldsymbol{\alpha}$ has the components $\alpha_x = \alpha_y = \alpha_\perp$, $\alpha_z = \alpha_\parallel$. It turned out that in an MNF with frozen-in magnetiza-

tion, fast and slow magnetosonic waves and Alfven-type waves can propagate.

The propagation velocities of fast c_f and slow c_s magnetosonic waves are determined by the formula

$$c_{f,(s)} = \frac{c_0}{\sqrt{2}}\sqrt{(1 + B_1 - A_1 \pm \sqrt{B_2 + B_3 - 2A_1 + A_2 - D})}. \quad (47)$$

The plus sign corresponds to the velocity of a fast magnetosonic wave, and the minus sign, to a slow one. This formula has been written for a change in angle ϑ in the limits from 0 to 90°. Here, the following notations were introduced:

$$B_1 = a_1(1+\beta)\cos^2\vartheta,$$

$$B_2 = [1 - a_1(1-\beta)\cos^2\vartheta]^2, \quad \beta = \beta_{\|}/\beta_{\perp},$$

$$B_3 = a_1(1-\beta)\sin^2 2\vartheta, \quad a_1 = m_0^2\beta_{\perp}/c_0^2,$$

$$a_2 = \rho_0 m_0 \alpha_{\perp}/c_0^2, \quad \alpha = \alpha_{\|}/\alpha_{\perp},$$

$$A_1 = 2a_2(\sin\vartheta + \alpha\cos\vartheta)\cos\vartheta,$$

$$A_2 = 4a_2^2(1+\alpha^2)\cos^2\vartheta,$$

$$D = 4a_1a_2(1-\beta)(\sin\vartheta - \alpha\cos\vartheta)\cos^3\vartheta.$$

The propagation velocity of an Alfven-type wave is determined by the relation

$$c_A = m_0\sqrt{\beta_{\perp}}\cos\vartheta. \quad (48)$$

In the examined Alfven-type waves, magnetization oscillates in contrast to an Alfven wave propagating in the liquid with infinitely large conductivity in which the intensity of magnetic field frozen into a liquid oscillates.

In the limit of zero magnetization, from (47) it follows that a fast magnetosonic wave passes to a common sound wave, and the velocity of a slow magnetosonic wave and an Alfven-type wave turn to zero. Figure 7 shows the qualitative character of the angle dependences of ultrasound velocity in an MNF predicted by the present theory. To calculate from formula (47) the velocity of a fast magnetosonic wave, the following parameter values were used: $c_0 = 10^5$ cm/s, $\rho_0 = 1$ g/cm^3, $m_0 = 20$ G. Curve *1* describes the ultrasound

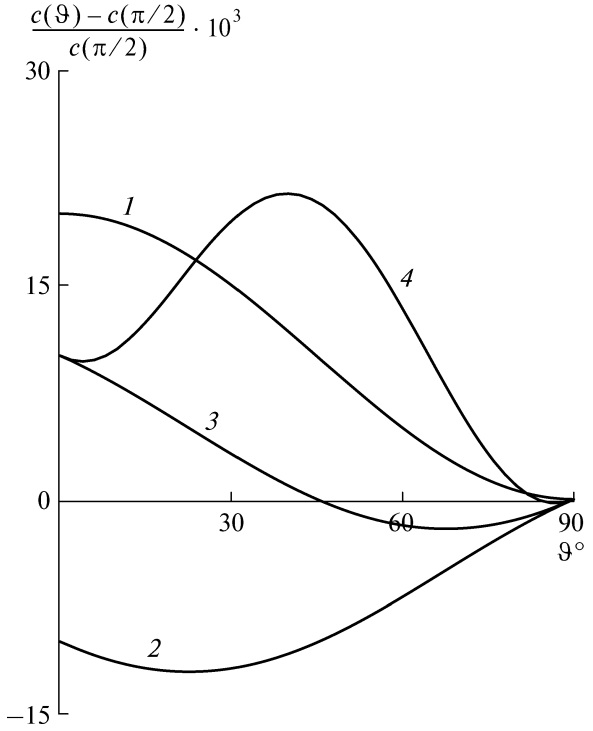

Fig. 7. Theoretical angle dependences of ultrasound velocity.

velocity anisotropy due only to the magnetoelastic mechanism ($\beta_{\|} = \beta_{\perp} = 10^6$ g/cm^3); curve *2*, due only to the magnetostrictive mechanism ($\alpha_{\|} = \alpha_{\perp} = 5 \times 10^6$ E cm^3/g); and curves *3* and *4* are the result of their combined manifestation at the indicated parameters—as well, curve *4* was obtained at $\beta_{\|} = 10^6$ g/cm^3, $\beta_{\perp} = 5 \times 10^6$ g/cm^3. It is easy to see that the presented qualitatively different theoretical angle dependences of ultrasound velocity were observed experimentally. Thus, the anisotropy of the elastic properties of MNFs results from both anisotropy of the magnetostrictive properties and anisotropy of magnetoelastic interaction.

Figure 8 shows a comparison of experimental results [14] with those calculated by relation (47) for a fast magnetosonic wave (solid curve) at the following parameters: $c_0 = 1.4356 \times 10^5$ cm/s, $\rho_0 = 1.166$ g/cm^3, $M_0 = 14.7$ G, $\beta_{\|} = 3.5 \times 10^5$ g/cm^3, $\beta_{\perp} = 9 \times 10^5$ g/cm^3.

In the case of the determining role of magnetoelastic interaction, for instance, in Fig. 8, expression (47) for the propagation velocities of magnetosonic waves takes the form

$$c_{f,(s)} = \frac{c_0}{\sqrt{2}}\sqrt{\left(1 + \frac{c_A^2}{c_0^2}(1+\beta)\right) \pm \sqrt{\left(1 + \frac{c_A^2}{c_0^2}(\beta - 1)\right)^2 + 4\frac{c_A^2}{c_0^2}(1-\beta)\sin^2\vartheta}}; \quad (49)$$

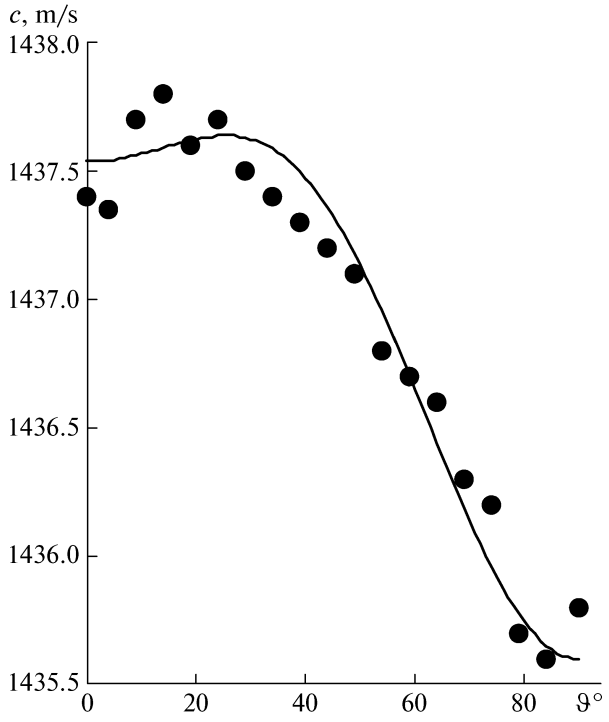

Fig. 8. Anisotropy of ultrasound velocity in a water-based MNF at $H = 8$ kA m^{-1}.

the propagation velocity of an Alfven-type wave is determined by (48). At $\vartheta = 0$, the propagation velocities of slow magnetosonic and Alfven-type waves coincide:

$$c_s = c_A = m\sqrt{\beta_\perp}. \quad (50)$$

It is important that the propagation velocities of slow magnetosonic and Alfven-type waves decrease, but in a different way, with an increase in angle ϑ, and at $\vartheta = \pi/2$, these waves do not propagate. It is necessary to take this into account when experimentally checking the suggested theory. Note that formulas (25) and (38) are quite close in structure to (50), but in the framework of the considered theory, a wave whose velocity is determined by expression (25) is an Alfven-type wave, and a wave whose velocity is determined by relation (38) is a slow magnetosonic wave. We also point out [74], in which the existence of a transverse wave in an uncompressed MNF was predicted, the velocity of which was determined by a relation coinciding with (25). In [75], the eigenvectors were calculated for the hydrodynamic modes of an MNF, in which only the magnetoelastic mechanism was taken into account, and it was shown that an Alfven-type wave is transverse, and fast and slow magnetosonic waves are mixed plane-polarized.

The predicted slow magnetosonic wave in an MNF has not been found to date.

However, the authors of [76] discovered experimentally the propagation of fast and slow waves in a magnetized suspension consisting of glycerin and spherical iron particles. They discussed the discovered slow magnetosonic wave using the Biot theory, which describes wave propagation in a porous body saturated with the liquid. The fallibility of this explanation by the Biot theory was pointed out in [77], since a slow wave propagates only when there is an external magnetic field, and the authors offered another explanation on the existence of a slow wave using a theory that they had developed earlier [64]. According to [64], in a magnetic fluid, there should exist a new elastic mode due to longitudinal vibrations in chains of magnetic particles, and it should not be a hydrodynamic mode, since a boundary frequency exists lower than which this mode is not excited. Experimental results [76] were described in [73] using the theory of wave propagation in a magnetic fluid with frozen-in magnetization. The suspension studied in [76] was prepared by addition of spherical iron particles to glycerin, the size of which were in the limits of 3–25 μm. The measuring cell with the suspension was placed into a magnetic coil, the current force in which varied from 0 to 35 A. The angle was equal to zero. The measuring cell had a diameter of 3 cm, and its length varied from 0 to 60 cm. In the absence of a magnetic field, only a fast magnetosonic wave was observed. The values of the propagation velocities of fast and slow magnetosonic waves, as well as the magnetic field strength at which they were measured, were determined from the graphs of [76]. These data are given in Table 3.

To apply relation (50), it is necessary to bear in mind the dependence, given in [76], of the iron particle concentration in the region of the acoustic channel on the size of the magnetic field strength. The existence of such a dependence can be explained by manifestation of the force of dipole–dipole repulsion of

Table 3. Properties of a magnetized suspension

H, G	60	130	180	250	310	370	430	490
c_s, m/s	35.5	38.5	40	42.5	44.5	45.5	46.5	47.5
c_f, m/s	1320	1560	1680	1740	1760	1800	1820	1850
ϕ_{ch}	0.167	0.113	0.090	0.072	0.064	0.059	0.056	0.054
m, G cm^3/g	121.5	96.7	83.7	71.5	65.2	61.3	59.0	57.6
$\beta_\perp \times 10^{-3}$, g/cm^3	0.85	1.56	2.28	3.53	4.67	5.51	6.22	6.80

neighboring particle chains; as well, with an increase in the strength of the magnetizing field, the lengths of chains increase and, consequently, the force of repulsion between them increases. According to [76], an analytical expression describing the dependence of the volumetric concentration of particles in the region of wave propagation on the magnetic field strength has the form

$$\phi_{ch} = (\phi - \phi_{sat})\exp(-dH) + \phi_{sat},$$

where $\phi_{sat} = 0.052$, $d = 0.0091$ G^{-1} [76]. The density of the suspension was calculated from the formula $\rho = (1 - \phi_{sat})\rho_g + \phi_{sat}\rho_{Fe}$, where $\rho_{Fe} = 7.88$ g/cm^3, $\rho_g = 1.261$ g/cm^3 are the densities of iron and glycerin, respectively. To estimate the specific magnetization, the simple formula $m = \phi_{ch}M_s/\rho$ was used. Here, $M_s = 1714$ G is the saturation magnetization of iron. With the use of (50), the values of parameters $\beta_\perp$ were determined, which proved to be two to three orders lower than for the MNF. Estimates show that in an MNF, the propagation rate of a slow magnetosonic wave is on the order of $c_s \simeq 100$ m/s. It is possible that such a small velocity of these waves is the very reason that slow magnetosonic waves have still not been found experimentally.

ACKNOWLEDGMENTS

In concluding, I would like to express sincere gratitude to Profs. B.U. Felderhof and P.A. Eminov for critical remarks and helpful advice.

REFERENCES

1. R. Rosensweig, *Ferrohydrodynamics* (Cambridge Univ. Press, New York, 1985; Mir, Moscow, 1989).
2. P. De Genes and P. A. Pincus, Phys. Condens. Mater. **11**, 189 (1970).
3. M. I. Shliomis, Usp. Fiz. Nauk **112**, 427 (1974) [Sov. Phys. Usp. **13**, 153 (1970)].
4. B. I. Pirozhkov, Yu. M. Pushkarev, and I. V. Yurkin, in *Sci. Essays of Perm. State Ped. Univ., Hydrodynamics* (Perm, 1976), pp. 164–166 [in Russian].
5. D. Y. Chung and W. E. Isler, Phys. Lett. **61**, 373 (1977).
6. V. E. Fertman and A. D. Solodukhin, in *Convection and Waves* (ITMO AN BSSR, Minsk, 1977), pp. 64–68 [in Russian].
7. V. M. Polunin and H. M. Ignatenko, Magn. Gidrodin., No. 3, 138 (1980).
8. P. P. Prokhorenko, A. R. Baev, and V. K. Rakhuba, Vestn. AN BSSR, Fiz. Tekh., No. 5, 88 (1981).
9. P. P. Prokhorenko, A. R. Baev, and E. M. Seregin, Vestn. AN BSSR, Fiz. Tekh., No. 1, 88 (1983).
10. K. X. Mansurov and V. V. Sokolov, Magn. Gidrodin., p. 63 (1987).
11. K. X. Mansurov and V. V. Sokolov, Magn. Gidrodin., No. 2, p. 25 (1988).
12. Yu. S. Alekhin, in *Proc. of the 3rd All-Union Symp. on Physics of Magnetic Liquids* (Stavropol, 1986), pp. 5–6.
13. N. Hornowski, A. Skumiel, and Ì. Labowski, Mol. Quantum Acoust. **61**, 41(2003).
14. T. Hornowski, in *Acousto-Optics and Applications,* Ed. by A. Linde, B. J. Sicorska, and A. Sliwinski, Proc. of SPIE, Vol. 5828 (SPIE, WA, Bellingam, 2005), pp. 205–211.
15. V. V. Sokolov and V. V. Nadvoretskiĭ, Magn. Gidrodin. **7**, 270 (1994).
16. S. M. Rytov, V. V. Vladimirskiĭ, and M. Galanin, Zh. Éksp. Teor. Fiz. **5**, 614 (1938).
17. R. J. Uric, JASA, No. 3, 283 (1948).
18. V. V. Gogosov, S. I. Martynov, S. N. Tsurikov, and G. A. Shaposhnikova, Magn. Gidrodin., No. 2, 19 (1987).
19. V. V. Gogosov, S. I. Martynov, S. N. Tsurikov, and G. A. Shaposhnikova.
20. V. M. Polunin, Akust. Zh. **31**, 234 (1985) [Sov. Phys. Acoust. **31**, 135 (1985)].
21. V. M. Polunin and A. A. Roslyakova, Magn. Gidrodin., No. 4, 59 (1985).
22. V. V. Sokolov, Izv. AN SSSR, Ser. Fiz., No. 6, 1057 (1987).
23. V. V. Gogosov, V. A. Naletova, and G. A. Shaposhnikova, in *Achievements of Science and Technology. Mechanics of Liquid and Gas* (VINITI, Moscow, 1981), vol. 16, pp. 76–208 [in Russian].
24. B. U. Felderhof, Phys. Rev. E, No. 3, 3848 (2000).
25. B. U. Felderhof, Phys. Rev. E, 0635021 (2001).
26. R. Rozensweig, J. Chem. Phys. **121**, 1228 (2004).
27. D. Y. Chung and W. E. Isler, J. Appl. Phys. **43**, 1809 (1978).
28. V. V. Sokolov, Magn. Gidrodin., No. 4, 136 (1986).
29. D. Chung and W. Å. Isler, IEEE Trans. Magn. **14**, 984 (1978).
30. N. M. Ignatenko, A. A. Rodionov, and V. M. Polunin, Izv. Vyssh. Uchebn. Zaved., Ser. Fiz., No. 4 (1983).
31. B. M. Berkovskiĭ, V. G. Bashtovoĭ, and V. M. Polunin, Magn. Gidrodin., No. 1, 69 (1986).
32. K. Gotoh and D. J. Chung, Phys. Soc. Jpn. **53**, 2521 (1984).
33. D. Chung and W. Isler, J. Appl. Phys. **43**, 1812 (1978).
34. S. Taketomi, J. Phys. Soc. Jpn. **55**, 838 (1986).
35. M. Kashparkova, Magn. Gidrodin., No. 1, 47 (1991).
36. V. V. Sokolov and V. V. Nadvoretsky, in *Proc. of the Nordic Acoustical Meeting, June 6–8, 1994*, Ed. by H. S. Olesen (Aarhus, 1994), pp. 461–466.
37. V. V. Nadvoretskiĭ and V. V. Sokolov, Magn. Gidrodin. **33** (1), 36 (1997).
38. J. Happel and H. Brenner, *Low Reynolds Number Hydrodynamics* (Prentice-Hall, Englewood Cliffs, NJ, 1965; Mir, Moscow, 1976).
39. A. S. Ahuja and W. R. Hendee, J. Acoust. Soc. Am. **63**, 1074 (1978).
40. D. Y. Chung, H. Z. Hung, and J. X. Lin, J. Magn. Magn. Mat. **39**, 111 (1983).
41. A. Jozefczak, M. Labowski, and A. Skumiel, J. Magn. Magn. Mater. **252**, 356 (2002).

42. A. Jozefczak, J. Magn. Magn. Mater. **256**, 267 (2003).
43. M. Motozawa and T. Sawada, Int. J. Mod. Phys. B **21**, 4914 (2007).
44. A. Jozefczak and A. Skumiel, J. Phys. Condens. Matter **18**, 1869 (2006).
45. M. Shliomis, M. Mond, and K. Morozov, Phys. Rev. Lett., No. 074505, 1 (2008).
46. S. P. Dmitriev, A. E. Luk'yanov, and V. V. Sokolov, Magn. Gidrodin., No. 3, 138 (1985).
47. S. P. Dmitriev and V. V. Sokolov, in *Proc. of the 6th Intern. Conf. on Magn. Fluids* (Paris, 1992). pp. 412–413.
48. S. P. Dmitriev and V. V. Sokolov, Akust. Zh. **43** (3), 123 (1997) [Acoust. Phys. **43**, 353 (1997)].
49. M. Motozawa, Y. Matsumoto, and T. Sawada, ISME Int. J. **48**, 471 (2005).
50. B. I. Kuzin and V. V. Sokolov, Akust. Zh. **40**, 689 (1994) [Acoust. Phys. **40**, 611 (1994)].
51. V. V. Sokolov and B. I. Kuzin, in *Proc. of the Nordic Acoustical Meeting, June 6–8, 1994*, Ed. by H. S. Olesen (Aarhus, 1994), pp. 467–470.
52. T. Sawada, H. Nishiyaraa, and T. Tabata, J. Magn. Magn. Mater. **252**, 186 (2002).
53. I. É. Ovchinnikov and V. V. Sokolov, Akust. Zh. **55** (2), 1 (2009) [Acoust. Phys. **55**, 359 (2009)].
54. B. I. Pirozhkov and M. I. Shliomis, in *Proc. of the 9th All-Union Acoust. Conf.* (Moscow, 1977), pp. 123–126.
55. Yu. L. Raĭkher and I. G. Shaposhnikov, *On Spectrum of Own Oscillations of Ferromagnetic Liquid* (Sverdlovsk, 1977) [in Russian].
56. V. M. Zaĭtsev and M. I. Shliomis, Prikl. Matem. Teor. Fiz., No. 5, 11 (1969).
57. M. I. Shliomis, Zh. Éksp. Teor. Fiz. **61**, 2411 (1971) [Sov. Phys. JETP **34**, 1291 (1971)].
58. J. B. Hubbard and P. J. Stiles, J. Chem. Phys. **84**, 6955 (1986).
59. F. V. Bunkin, A. I. Lipkin, and G. A. Lyakhov, Pis'ma Zh. Tekh. Fiz. **9**, 714 (1983) [Sov. Tech. Phys. Lett. **9**, 307 (1969)].
60. K. Henjes, Phys. Rev. E **50**, 1184 (1994).
61. H. W. Muller and M. Liu, Phys. Rev. Lett. **89**, 0672011 (2002).
62. J. D. Parsons, J. Phys. D.: Appl. Phys. **8**, 1219 (1975).
63. S. Taketomi, J. Phys. Soc. Jpn. **54**, 102 (1985).
64. H. Plainer and H. R. Brand, J. Magn. Magn. Mater. **85**, 125 (1990).
65. V. V. Tolmachev, A. M. Golovin, and V. Potapov, *Thermodynamics and Electrodynamics of Continuous Media* (Mosk. Gos. Univ., Moscow, 1988) [in Russian].
66. V. V. Sokolov and V. V. Tolmachev, Magn. Gidrodin. **32**, 313 (1996).
67. M. A. Mikaélyan, Usp. Fiz. Nauk **168**, 1331 (1998) [Phys. Usp. **41**, 1219 (1998)].
68. V. V. Sokolov and V. V. Tolmachev, Magn. Gidrodin. **32**, 318 (1996).
69. N. G. Van Kampen and B. U. Felderhof, *Theoretical Methods in Plasma Physics* (North-Holland, Amsterdam, 1967), p. 215.
70. V. V. Sokolov and V. V. Tolmachov, in *Proc. of the 14th Intern. Riga Conf. on Magn. Hydrodyn.* (Jurmala, 1995), p. 168.
71. V. V. Sokolov and V. V. Tolmachev, Dokl. Akad. Nauk **54**, 488 (2009) [Dokl. Phys. **54**, 325 (2009)].
72. V. V. Sokolov and V. V. Tolmachov, in *Proc. of the Sev. Intern. Conf. on Magnetic Fluids* (Bhavnagar, 1995), pp. 194–195.
73. V. V. Sokolov and V. V. Tolmachev, Akust. Zh. **43**, 1 (1997) [Acoust. Phys. **43**, 92 (1997)].
74. S. Bastrukov and P. Y. Lai, Chin. J. Phys. **37**, 325 (1999).
75. V. V. Sokolov and I. E. Ovchynnikov, in *Proc. of the 5th Intern. Pamir Conf. on Fundamental and Applied MHD, France* (Ramatuelle, 2002), Vol. 2, pp. 81–84.
76. Y. Nahmad-Molinari, C. A. Arancibia-Bulnes, and J. Ruis-Suares, Phys. Rev. Lett. **82**, 727 (1999).
77. H. R. Brand and H. Pleiner, Phys. Rev. Lett. **86**, 1385 (2001).

Translated by A. Carpenter